

# Structural features of inclusion complexes of $\gamma$ -cyclodextrin with various polymers

Junka Kawasaki<sup>a</sup>, Daisuke Satou<sup>a</sup>, Tomomi Takagaki<sup>a</sup>, Takashi Nemoto<sup>b</sup>, Akiyoshi Kawaguchi<sup>a,\*</sup>

<sup>a</sup> Faculty of Science and Engineering, Ritsumeikan University, 1-1-1 Nojihigashi, Kusatsu, Shiga 525-8577, Japan

<sup>b</sup> The Institute for Chemical Research, Kyoto University, Uji, Kyoto 611-0011, Japan

Received 12 July 2006; received in revised form 16 November 2006; accepted 6 December 2006

Available online 12 January 2007

---

## Abstract

The crystalline structures of inclusion complexes of  $\gamma$ -cyclodextrin ( $\gamma$ -CD) with poly(ethylene glycol), poly(ethylene adipate), poly(propylene glycol) and poly(isobutylene) were studied by electron microscopy, in combination with X-ray diffraction works and measurements of thermal properties by DSC and TGA. The crystalline structure of as-prepared complexes was tetragonal and its cell dimensions were  $a = b = 2.380$  nm and  $c = 1.48$  nm. When an as-prepared sample was dried in a vacuum at room temperature, the tetragonal modification was transformed into the monoclinic one with the projected cell dimensions of  $a = 1.75$ ,  $b = 1.36$  nm and  $\gamma = 110^\circ$ . The transformation occurred by progressive ‘shifting’ of rows of polymer necklaces in the [110] direction along the (110) plane in an original tetragonal lamellar crystal. Complexes lost weight by 10–15% in the process of heating up to 140 °C. The tetragonal crystalline modification was transformed into the hexagonal one, and concurrently, the X-ray diffraction profiles of annealed complexes were broadened. When a sample was dried in a vacuum at room temperature or annealed at high temperatures, followed by exposure to water vapor, the original tetragonal crystalline structure was recovered, restoring the original degree of orientation of crystallites in the sample. When water molecules were removed, the lateral stacking order of  $\gamma$ -CD–polymer complexes was destroyed, but the basic necklace structure in which polymer chains threaded through the cavity of  $\gamma$ -CD rings’ structure could be retained.

© 2007 Elsevier Ltd. All rights reserved.

**Keywords:**  $\gamma$ -Cyclodextrin; Electron microscopy; Inclusion complex

---

## 1. Introduction

For a long time, it is known that  $\alpha$ -,  $\beta$ - and  $\gamma$ -cyclodextrins (CDs) consisting of six, seven and eight glucopyranose units, respectively, form complexes with various kinds of organic molecules, incorporating them as guests within their cavity. Potential use of complexes of  $\gamma$ -CD with organic compounds, including polymers, was reviewed by Szejtli [1]. It is also interesting that  $\gamma$ -CDs are able to incorporate metal ions as ligands to prepare magnetic nano-particles [2]. Harada and Kamachi [3] first found that poly(ethylene glycol) thread  $\alpha$ -CD rings to form polymer/cyclodextrin complex. Since their finding of inclusion complex formation of polymer chains with

$\alpha$ -CD, a large number of studies on inclusion complexes of  $\alpha$ -,  $\beta$ - and  $\gamma$ -CDs with various polymers have been reported. Polymer main chains threaded the cavity of CDs to form the so-called molecular necklace [4], and side chains of branched polymer did as well [5]. When branched polymers with poly(ethylene oxide) side chains were mixed with the solution of  $\alpha$ -CD in water, the side chains skewered  $\alpha$ -CD rings to form complexes so that “gelation” occurs [6]. In these observations, the inclusion complexes were prepared in the liquid phase, i.e. by mixing the solution of CD in water with the polymer solution or with molten polymer at a high temperature or by mixing both CD and polymer solutions in organic solvents [7]. Recently, inclusion complexes of  $\alpha$ -CD with poly(ethylene glycol) (PEG) were formed through ‘solid-state process’, that is, PEG threaded  $\alpha$ -CD to form complexes when  $\alpha$ -CD was mixed and stirred with PEG [8]. Thus, various preparation methods

---

\* Corresponding author. Fax: +81 (0)775612659.

E-mail address: [akiyoshi@se.ritsumeiki.ac.jp](mailto:akiyoshi@se.ritsumeiki.ac.jp) (A. Kawaguchi).

to make inclusion complexes are developed, and application of ability of CDs to form complexes is groped for.

As for inclusion complexes of  $\gamma$ -CD with various polymers, their formation method and characteristic were also studied [9–27]. In all cases, inclusion complexes comprise the channel type of column. In inclusion complexes with poly(ethylene adipate) [12], poly(caprolactone) [17] and poly(ethylene glycol) [10], it was reported that the two polymer chains threaded the cavity of  $\gamma$ -CDs to form a column, in which their rings are stacked in sequence in head-to-head or tail-to-tail contact. On the other hand, a model in which a single chain was incorporated as guest was proposed for the inclusion complex with poly(isobutylene) [9]. It is revealed further by IR spectroscopy and NMR measurement that guest polymers thread through the cavity of  $\gamma$ -CDs, taking the planar conformation [17]. Thus, the molecular models of incorporating manner of polymer chain(s) within  $\gamma$ -CD cavity were proposed. However, the crystalline structure, or the lateral packing of resulting columns of  $\gamma$ -CD inclusion complexes with polymers as well as those of  $\alpha$ - and  $\beta$ -CDs was less examined [28,29] although the crystalline structures of  $\gamma$ -CD complexes with low molecular weight molecules were studied in detail [30–35]. It is because a crystal of inclusion complex with polymers, large enough to be suitable for X-ray analyses, cannot be prepared. For studies on small crystallites, electron microscopy is useful.

In the previous paper, it was reported that  $\gamma$ -CD formed a superlattice with poly(ethylene adipate) [29]. By further studies using X-ray diffraction and electron microscopy, it was found that the superlattice was not real but due to misinterpretation of electron diffraction patterns and that the real structure resulted from the repeated twinning, which was devised elaborately during removal of water hydrates from an inclusion complex crystal. Here, on the basis of additional data from DSC and TGA, the crystalline structures of  $\gamma$ -CD with various polymers are featured, in comparison with the crystallographically well-defined complexes with low molecular weight guest molecules.

## 2. Experiments

$\gamma$ -Cyclodextrin ( $\gamma$ -CD) and polymer samples except poly(ethylene adipate) (PEA) were commercially available. A purity of  $\gamma$ -CD (Wako Pure Chemicals Inc. Ltd.) was 97%, and average molecular weights of poly(ethylene glycol) (PEG) (Tokyo Kasei Co. Ltd.), poly(propylene glycol) (PPG) (viscous liquid, Wako Pure Chemicals Inc. Ltd.) and poly(isobutylene) (PIB) (viscous liquid, Polysciences Inc.) were 2000, 1000 and 1350, respectively. Poly(ethylene adipate) was synthesized according to the method in Ref. [12]. As-synthesized material was used without fractionation as it was. Molecular weight was unknown, but the degree of polymerization was not so high because the material was pasty at room temperature.

To prepare complexes of  $\gamma$ -CD with these polymers, the procedures reported in Refs. [2,3] were adopted basically. A solution of  $\gamma$ -CD in water at a concentration of 10 wt% was prepared. The solution was mixed with the 10 wt% solutions of PEG in water with the ratio of 1:1 in volume and stirred

at room temperature. Since other polymers are insoluble in water, the excess of the  $\gamma$ -CD solution in water was put together with these polymers in a glass tube and stirred at a high temperature [9–11], e.g. about 50 °C. In all cases, complex crystals were precipitated during stirring.

Crystals thus precipitated were observed by an electron microscope by JEOL (100C), which was operated at 100 kV. For X-ray studies, crystals in suspension were sedimented and filtered to make a mat. X-ray photographs of the mat was taken with imaging plates, using a generator which was operated at 40 kV and 30 mA, and diffraction profiles of powders were also obtained by a diffractometer. Annealing of the crystals was carried out in vacuum.

Thermal properties were examined by differential scanning calorimetry (DSC) and thermo gravimetric analysis (TGA). DSC and TGA measurements were done at a heating rate of 10 °C/min.

## 3. Results

### 3.1. Thermal behaviors

Fig. 1 shows DSC thermograms of raw  $\gamma$ -CD and of inclusion complexes with various polymers. Though the individual DSC thermograms exhibit the behavior characteristic of respective complexes, the endothermic peak at around 90 °C is commonly observed in curves (a), (b), (d) and (e), and one at around 280 °C in curves (a), (b), (c) and (e). In inclusion complexes of  $\gamma$ -CD with other polymers [14,16,18,20,22,23,25,26,36], endothermic peak or base shift was observed in the same temperature range in their DSC thermograms. Fig. 2 shows the TG thermograms of inclusion complexes with various polymers. Among all TG thermograms, there is a common feature that the weight of sample decreases over the temperature range of around 50–120 °C, i.e. by 8–10% for  $\gamma$ -CD and complexes of PEO, 12% for complexes of PIB and PPG and 14% for complexes of PEA. In inclusion complexes with other polymers [14,16,18,20–23,36],

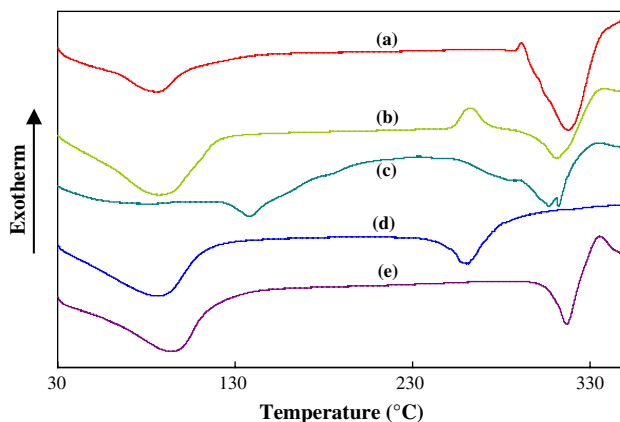


Fig. 1. DSC curves of (a)  $\gamma$ -CD and its inclusion complexes with (b) poly(ethylene glycol), (c) poly(propylene glycol), (d) poly(ethylene adipate) and (e) poly(isobutylene). Heating rate is 10 °C/min.

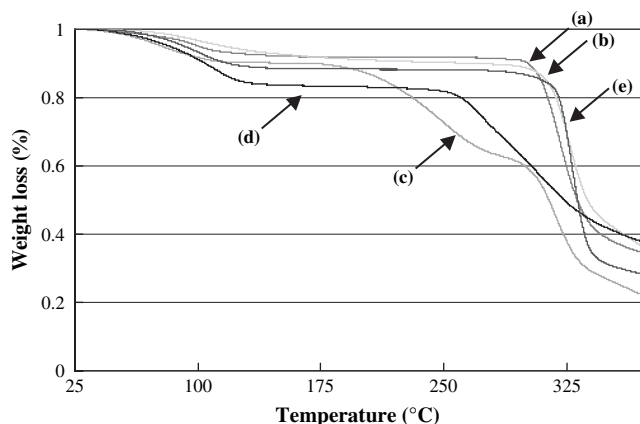


Fig. 2. TG thermograms of (a)  $\gamma$ -CD and its inclusion complexes with (b) poly(ethylene glycol), (c) poly(propylene glycol), (d) poly(ethylene adipate) and (e) poly(isobutylene). Heating rate is 10 °C/min.

the weight loss was observed in this temperature range of their TA thermograms. This temperature range just corresponds to the endothermic peaks of DSC curves in Fig. 1. As seen from a review by Giordano et al. [37], the same thermal behavior has been observed on a vast number of cyclodextrin complexes with organic compounds. It is to be noted that the thermal behavior is common to all inclusion complexes of cyclodextrins.

The thermo gravimetric curve (a) in Fig. 2 shows that  $\gamma$ -CD lost further its weight at around 300 °C. Though we have no evidence by chemical analyses, it is natural that the weight loss should occur by thermal decomposition of  $\gamma$ -CD [26]. Similarly, in other complexes, the endothermic peaks in the corresponding temperature range in Fig. 1 were caused by the thermal destruction of polymer and  $\gamma$ -CD. Such thermal loss of weight was observed in other TG works [14,16,18,20–23]. In curve (d) of  $\gamma$ -CD–PEA of Fig. 2, the further weight loss started at around 250 °C, which corresponds to the endothermic peak in Fig. 1, at a temperature lower than this, the weight loss of  $\gamma$ -CD–PPG complex started. Such weight loss at three stages occurred in heating other polymer complexes [16,21,22]. In contrast, the weight of  $\gamma$ -CD–PEG complex started to lose weight at around 300 °C. It is considered, thus, that in the cases of  $\gamma$ -CD–PEA and  $\gamma$ -CD–PPG systems, the break down of complex occurred at a lower temperature by degradation of PEA and PPG threads. The TG thermograms of  $\gamma$ -CD–PEG and  $\gamma$ -CD–PIB exhibited the essentially similar thermogravimetry behaviors to that of  $\gamma$ -CD implies that these complexes are stable up to high temperatures.

From above results, it is found that since  $\gamma$ -CD is stable up to 300 °C, the weight loss of  $\gamma$ -CD and its inclusion complexes up to 120 °C should arise from removal of water molecules from the samples. Some water molecules only adhered physically to the sample, and some were incorporated as hydrates between  $\gamma$ -CD rings and within their cavity in inclusion complexes, as detailed by structural analyses of the complexes with simple molecules [30–35]. Water molecules incorporated thus in a physically different way were not separated experimentally. Now, we shall assume that water molecules removed

in the heating process were all incorporated as hydrates. Thus, the weight loss of 15–18% implies that roughly speaking, 10–15 water molecules per  $\gamma$ -CD molecule were involved in crystals. This amount of hydrates is comparable to that of  $\gamma$ -CD clathrate with simple molecules, e.g. 12 and 17 hydrates in  $\gamma$ -CD/1-propanol clathrate [32,34,36].

### 3.2. X-ray diffraction analyses

Fig. 3 compares X-ray diffraction profiles of the powders of as-prepared  $\gamma$ -CD–PEG complexes and a powder sample dried overnight in a vacuum at room temperature. Reflections of the profile (a) are appropriately indexed on the basis of the tetragonal unit cell:  $a = b = 2.380$  nm and  $c = 1.48$  nm. The  $a$  and  $b$  cell dimensions are comparable to those of inclusion complexes with simple molecules [31–36] and proposed by Panovia et al. [28]. Of course, the diffraction profile is indexed on the basis of the unit cell obtained by them. The lattice parameters are re-examined later.

In the profile of dried sample in Fig. 3(b), in addition to the 200 reflection of as-prepared sample, two peaks with the lattice spacings of 1.29 and 1.10 nm are observed as indicated by curly bracket. The triplet of reflections was observed on the inclusion complex with *n*-propanol by Takeo and Kuge [38], and they referred to them only as an unknown structure. Similar changes in the X-ray diffraction profile are seen on the vacuum-dried inclusion complex with poly(methyl-methacrylate) although not so clear-cut as in the present profile [26]. The changes in profile clearly mean the transformation of the tetragonal crystalline form to another by removal of water molecules.

The reflection of the lattice spacing of 0.730 nm, which is indexed as 002 reflection on the present unit cell, remained in the dried sample. This implies that the ordered stacking of  $\gamma$ -CD rings in the channel type still holds in dried sample. However, as the diffraction profile (b) is broadened overall, the degrees of both stacking order of  $\gamma$ -CDs in a column of complex and lateral packing of columns of complexes decrease by

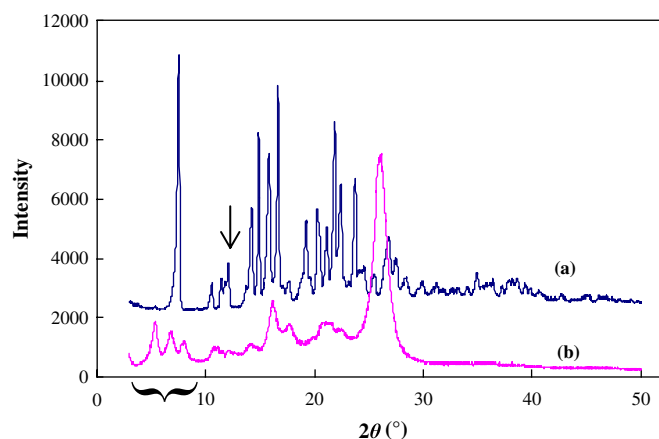


Fig. 3. X-ray diffraction profiles of the powder of  $\gamma$ -CD complexes with PEG: (a) as-prepared and (b) dried in a vacuum overnight at room temperature. The peak indicated with an arrow of profile (a) has a lattice spacing of 0.736 nm and is indexed as 002 reflection.

the transformation. When the vacuum-dried sample was exposed to water vapor, the same diffraction profile as that of as-prepared sample was reproduced as observed when heat-treated samples were exposed to water vapor (detailed below).

Fig. 4 shows X-ray diffraction photographs of a sedimented mat of  $\gamma$ -CD–PEG complexes, which was treated in various ways. In Fig. 4(b), broad reflections are observed. However, the arced reflections show that the crystalline order was still retained even after the mat was annealed at 140 °C although the degree of ordering becomes lower. It is to be noted that the temperature is just higher than the end temperature of the first weight loss in Fig. 2. Fig. 4(c) was taken from the mat which was annealed at a higher temperature, 240 °C, where the second weight loss started in Fig. 2. Reflections are more broadened. The degree of orientation of crystallites was deteriorated more.

Arrowed meridional reflections labeled as 1–5 in Fig. 4(a), with the lattice spacings of 1.656, 1.183, 0.835, 0.523 and 0.3941 nm, are indexed as 110, 200, 220, 410 and 530, respectively, on the basis of the above-mentioned tetragonal unit cell. From the indexing, we see that the  $c$  axis is oriented horizontally in X-ray diffraction pattern of Fig. 4. The equatorial reflection I has a lattice spacing of 0.736 nm. In the equator of Fig. 4(a), there are no observed reflections with a lattice spacing of 2.3 nm, which was observed by Panovia et al. [28] and indexed as the 001 reflection. Thus, we consider that the

reflection should be indexed as 002 reflection and estimate the  $c$  cell dimension at 1.47 nm. All diffraction profiles of  $\gamma$ -CD–polymer complexes are appropriately indexed.

X-ray photographs in Fig. 4(b') and (c') were taken from the samples, which were exposed to water vapor at around 90 °C after annealed at 140 and 240 °C, respectively. Both X-ray photographs resemble each other quite well. Further, it is amazing that the diffraction features of the photograph of the original mat are reproduced in both patterns: crystalline reflections are very sharp and their degree of arcing is quite similar to that of as-prepared mat. When hydrate water molecules were escaped from the crystals by heat treatment, the crystallinity of complexes was deteriorated. The fact that the crystalline order of complexes was recovered by exposing water vapor demonstrates that water molecules should play a fatal role for formation of inclusion complexes of  $\gamma$ -CD with polymers. Really, in inclusion complexes of  $\gamma$ -CD with simple molecules, water molecules are incorporated in registered positions as hydrates to form the crystalline structure [30–33]. Complementarily, it is pointed out here that X-ray photographs of inclusion complexes of  $\alpha$ -CD with PEG were not changed when they were annealed in the same manner at high temperatures.

Fig. 5 shows the X-ray diffraction profiles of the powder of  $\gamma$ -CD–PEA complex, which was treated similarly in various ways as in Fig. 4. The powders of complexes with PEO and PPG gave the similar profiles to those shown in Fig. 5,

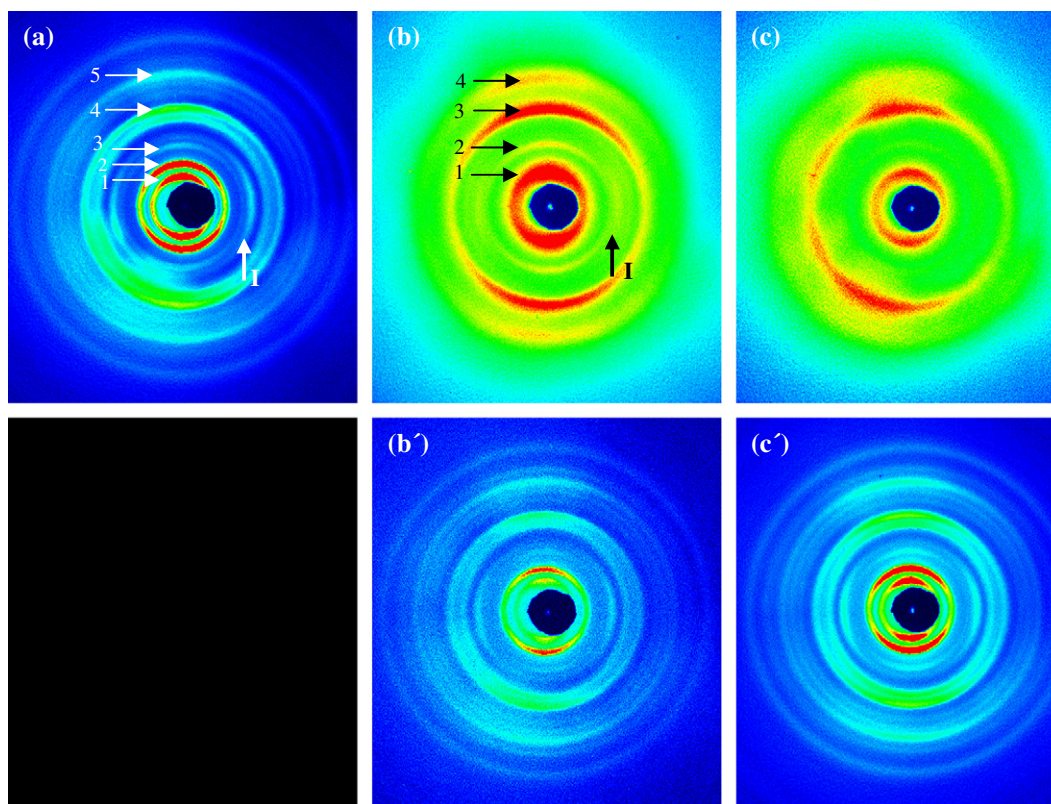


Fig. 4. X-ray diffraction photographs of the sedimented mat of inclusion complex of  $\gamma$ -CD with PEG: (a) as-prepared, and samples annealed at (b) 140 and (c) 240 °C, and (b') and (c') of the samples corresponding to (b) and (c), which were exposed to water vapor at 90 °C after annealed at respective temperatures. The sedimented mat was set horizontally, the normal to its surface being vertical. X-ray beam was incident parallel to the its surface and perpendicular to the figure.

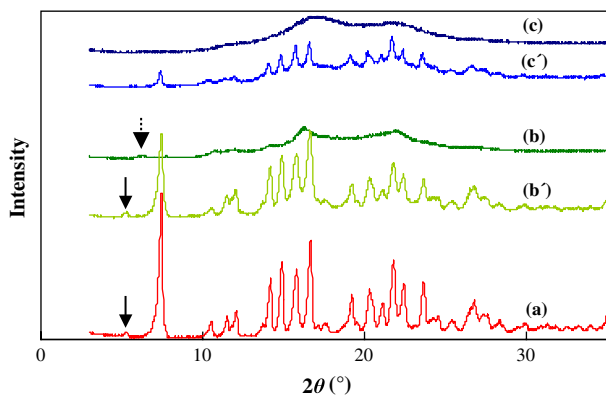


Fig. 5. X-ray diffraction profiles of various inclusion complex powders of  $\gamma$ -CD with poly(ethylene adipate): (a) as-prepared, and samples annealed at (b) 140 and (c) 240 °C, and (b') and (c') of the samples corresponding to (b) and (c), which were exposed to water vapor at 90 °C after annealed at respective temperatures.

corresponding to the respective heat treatments. From these profiles, we can confirm diffraction features and intensity relationship of reflections, which are discussed for  $\gamma$ -CD–PEO system on the basis of the X-ray photographs in Fig. 4. Table 1 shows the 110 lattice spacing of as-prepared inclusion complexes with various polymers.

Profile (b) in Fig. 5 was taken from a sample, which was annealed at a temperature just after the first weight loss ended in Fig. 2. This demonstrates that the crystallinity of the inclusion complex with PEA was lost as water molecules were further removed by heat treatment. It is also observed in inclusion complexes with other polymers that their diffraction profile became broad when complex samples were dried in vacuum [20,26]. Fig. 6 shows the X-ray diffraction profiles of powder samples of  $\gamma$ -CD–PIB complex, which were also prepared in the same way as in the case of  $\gamma$ -CD–PEO. It is to be noted that crystalline peaks from annealed  $\gamma$ -CD–PIB complexes, as indicated by a curly bracket in the profile (c) in Fig. 6, were still distinguishable although rather broadened. This implies that  $\gamma$ -CD–PIB complexes would be thermally durable to a high temperature. This is compatible to the observation that the TG thermogram kept plateau to 300 °C in Fig. 2(e). Of course, annealed  $\gamma$ -CD–PIB complexes also recovered the crystalline, sharp diffraction profiles when exposed to water vapor. Thus, since X-ray profiles were taken in the ambient condition, a trace of crystalline peaks in Fig. 6(c) could be caused by absorbing water molecules during measurement. It is to be stressed again that water molecules are inevitable to concrete the ordered structure of  $\gamma$ -CD complex with polymers.

Table 1  
The 110 lattice spacing of inclusion complexes of  $\gamma$ -CD with various polymers, obtained from powder X-ray diffraction patterns

Ann. temp (°C)	Polymer			
	PEO	PEA	PPG	PIB
As-prepared	1.675	1.653	1.617	1.629
140	1.698	1.675	1.654	1.606
240	1.692	1.709	1.641	1.628

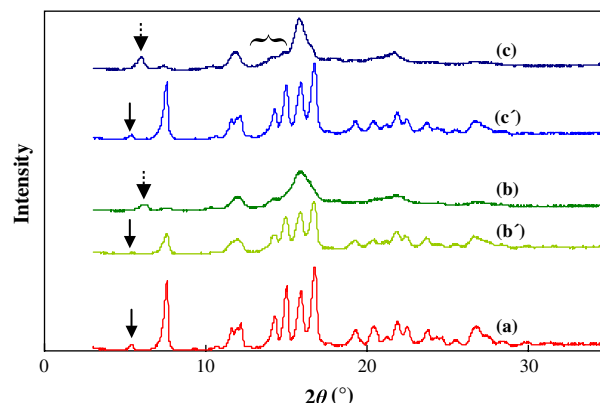


Fig. 6. X-ray diffraction profiles of the inclusion complex powder of  $\gamma$ -CD with PIB: (a) as-prepared, and the samples annealed at (b) 140 and (c) 240 °C, and (b') and (c') for the samples corresponding to (b) and (c), which were exposed to water vapor at 90 °C after annealed at respective temperatures.

### 3.3. Electron microscopy

In Fig. 7, electron diffraction patterns of  $\gamma$ -CD complex platelets with PEG, PEA, PPG and PIB are shown. The diffraction features of the complex of  $\gamma$ -CD with PEA are reported previously [29]. Here, the similar diffraction features are identified and commonly observed on these diffraction patterns of the  $\gamma$ -CD complexes with various polymers: if the superlattice would be real as described in Ref. [29],

1. the cell dimensions of its projected tetragonal cell on the  $a$ – $b$  basal plane would be  $a = b = 9.742$  nm, and
2. the subcell with cell dimensions of  $a_o = b_o = 1.657$  nm would be derived from the spots along the  $a^*$  and  $b^*$  axes.

It was found that the superlattice was not realized but was due to false indexing of electron diffraction. This is discussed in detail below.

Fig. 8(a) shows an electron micrograph of  $\gamma$ -CD complex with PEA, which was annealed at 140 °C. The crystal shape is rectangular. Basically, plate-like crystallites are tetragonal or rectangular in shape. Cracks run parallel to the edges. Since the surface of as-prepared platelet was smooth, cracks were caused by removal of water molecules by annealing [28]. Fig. 8(b) shows an electron diffraction pattern of a specimen, which was annealed at 140 °C followed by exposure to water vapor. The electron diffraction pattern of annealed specimens gave only amorphous halo. Such a spotty electron diffraction pattern as an as-prepared platelet gave was completely reproduced. By electron diffraction, it is ascertained that the original crystallinity of platelet could be recovered by exposing to water vapor. In the case of a  $\gamma$ -CD–PIB complex, an electron diffraction pattern as shown in Fig. 9 was often obtained even when annealed at a high temperature of 240 °C. The crystalline nature of a  $\gamma$ -CD–PIB complex could be retained up to a high temperature of 240 °C. Of course, the duration of crystallinity depends on the annealing time.

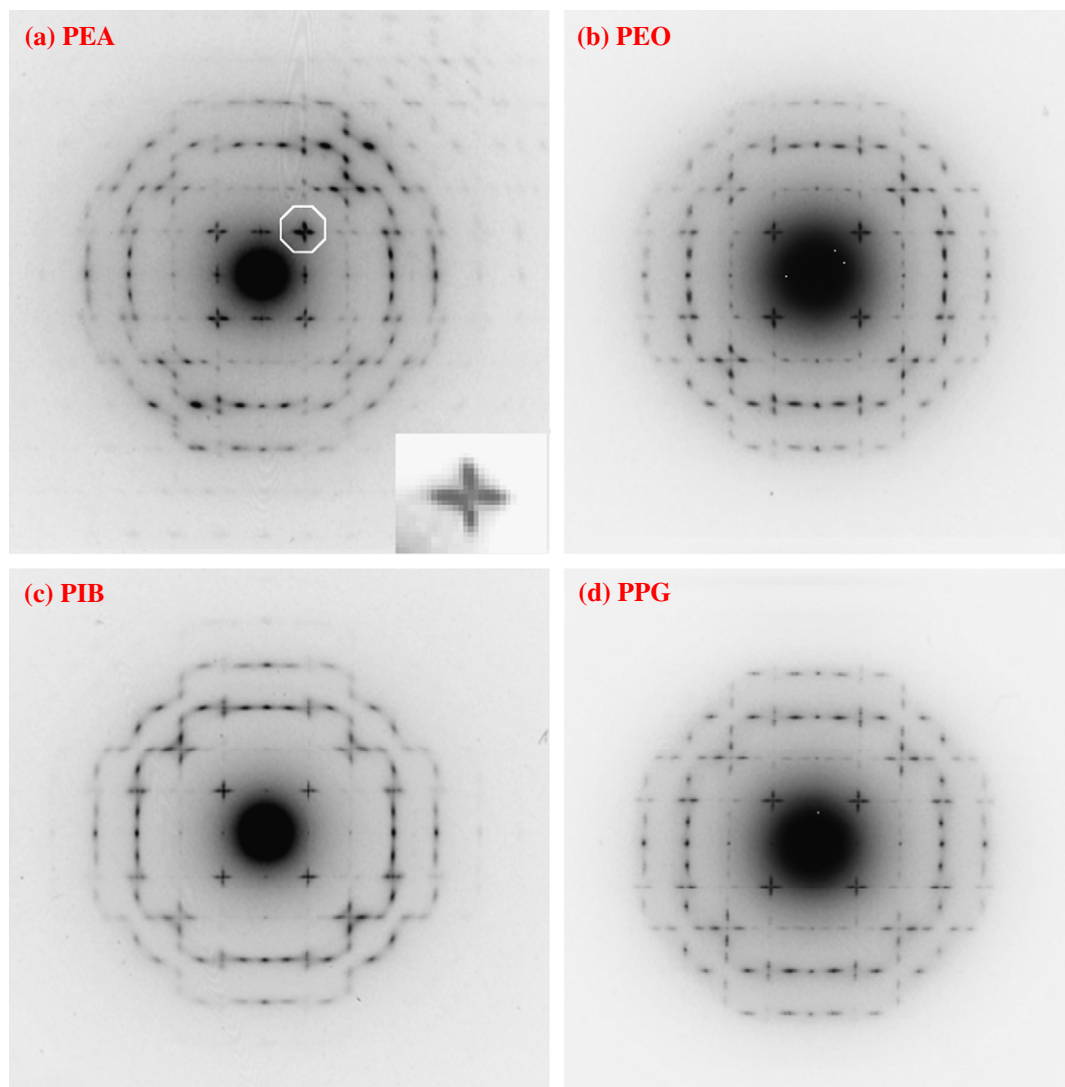


Fig. 7. Selected area electron diffraction patterns of inclusion complex crystals of  $\gamma$ -CD with (a) poly(ethylene adipate), (b) poly(ethylene glycol), (c) poly(isobutylene) and (d) poly(propylene glycol). The inset in (a) is a magnified image of the encircled part.

## 4. Discussion

### 4.1. Feature of tetragonal form

Harada et al. first reported that  $\gamma$ -CDs form the inclusion complexes with polymers, in which a polymer chain thread their rings to make a molecular necklace [2,3]. Panovia et al. showed that there were two modifications of  $\gamma$ -CD–PEO complex crystal; one was the tetragonal form for the as-prepared complex with water (named  $\gamma$ -CD–PEO–H<sub>2</sub>O) and the other was for the annealed sample without water (named  $\gamma$ -CD–PEO) but its crystal system was unknown [28]. Prior to these observation, Takeo and Kuge identified three crystalline forms of  $\gamma$ -CD–PEO complexes: the tetragonal form of as-prepared, hydrated complexes; the hexagonal form of dried, anhydrous complexes; the unknown one as mentioned above. In either of the tetragonal and hexagonal forms, complexes comprise  $\gamma$ -CDs aligned in the channel type, through the cavity of which guest polymers pass

[38]. The present analyses of X-ray diffraction patterns of as-prepared inclusion complexes with various polymers were explained on the basis of the tetragonal unit cell with the cell dimensions:  $a = b = 2.38$  nm and  $c = 1.472$  nm. The size of the  $a$ – $b$  projection of unit cell just corresponding to those of  $\gamma$ -CD–PEO–H<sub>2</sub>O, which were obtained by Takeo and Kuge and by Panovia et al. Thus, as for as-prepared samples, the molecular necklaces extended into columns were packed laterally into a tetragonal lattice with cell dimensions  $a = b = 2.380$  nm, independently of the kind of guest polymer (detailed later in Fig. 11).

The  $c$  cell dimensions of inclusion complexes of simple molecules [30–35] and of polyethylene oxide [28] were reported as 2.3 nm. It corresponds to the thickness of three  $\gamma$ -CD rings. It is made clear that in the  $\gamma$ -CD complexes with simple molecules which crystallize in the form of columns, so-called the channel type structure,  $\gamma$ -CD rings are stacked forming triplets with head-to-head and head-to-tail contacts along the  $c$  axis [34–36]. As observed the 001

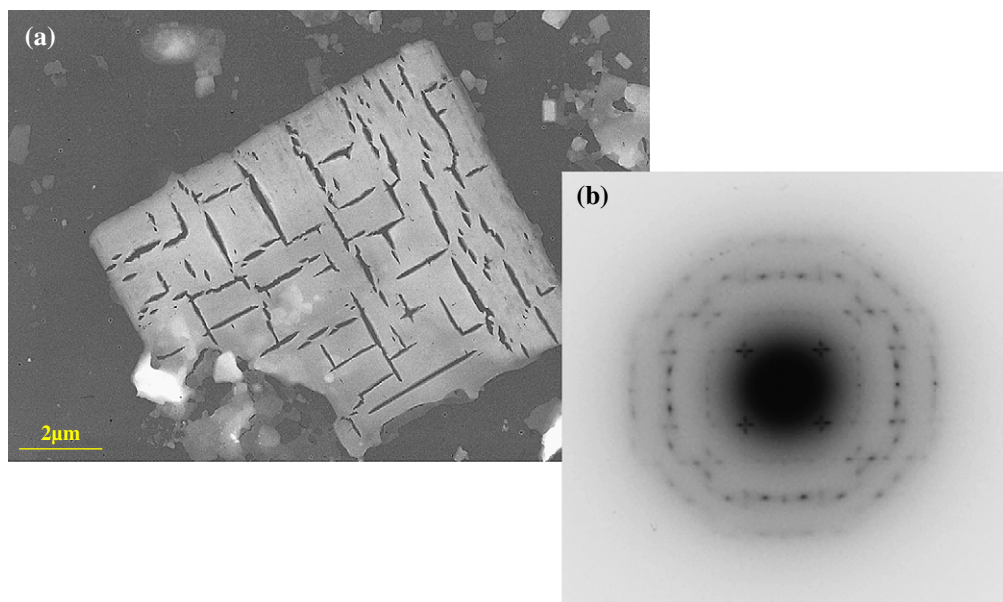


Fig. 8. (a) Electron micrograph of  $\gamma$ -CD complex with poly(ethylene adipate), which was annealed at 140 °C. (b) Selected area electron diffraction pattern of a inclusion complex crystal of  $\gamma$ -CD with PEA, which was annealed at 140 °C and subsequently exposed to water vapor at 90 °C.

reflection of the lattice spacing of 2.3 nm, Panovia et al. proposed that the stacking sequence of  $\gamma$ -CDs in the column involves the same head-to-head and head-to-tail contacts as

in the case of molecular complexes with simple molecules [28]. In the present work, the  $c$  cell dimension was estimated at 1.472 nm. It corresponds to the thickness of two  $\gamma$ -CD rings. This shows that  $\gamma$ -CD rings are stacked in a column, alternating the head-to-head and tail-to-tail contacts, as depicted in many references, for example, in Refs. [10,11,17,22,24,26].

The reflection with the lattice spacing ranging from 0.729 to 0.739, which is indexed as the 002 reflection, was also observed in the annealed inclusion complexes. It was found here that  $\gamma$ -CD rings were stacked in the channel type even in annealed complexes, retaining the similar stacking sequence to that of as-prepared inclusion complexes. In the inclusion complexes of  $\alpha$ -CD with PEO, the 001 reflections of 1.68 [28] and 1.56 nm [2] were observed. The 001 lattice spacings are corresponding to the double thickness of  $\alpha$ -CD ring. From this, it is considered that  $\alpha$ -CD rings are stacked in the necklace, alternating head-to-head and tail-to-tail contacts.

#### 4.2. Reversible transform into tetragonal form

The lattice spacings of arrowed meridional reflections in Fig. 4(b), labeled as 1–4 are 1.375, 0.828, 0.525 and 0.401 nm, respectively. The lattice spacings of reflections 2 and 3 are comparable to those of reflections 3 and 4 in Fig. 4(a). These reflections are attributed to the crystallites of the tetragonal form, which were not suffered from structural change by annealing. The lattice spacing of 1.375 nm of the reflection 1 is substantially smaller than that of the reflection 1 in Fig. 4(a) even though the angular resolution of the flat camera method (with the camera length 30.3 mm) is low. The diffraction profiles in Figs. 5 and 6 make it more clear. The reflection with the lattice spacing of  $\sim 1.6$  nm became less intense with increasing the annealing temperature and eventually disappeared (see the decrease in the peak indicated by a thin arrow

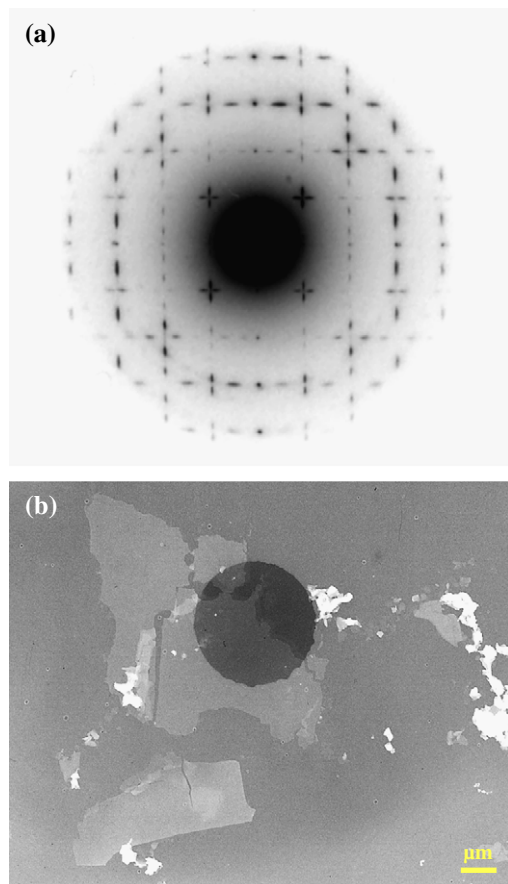


Fig. 9. (a) Selected area electron diffraction pattern and (b) corresponding electron micrograph of the inclusion complex of  $\gamma$ -CD with PIB, annealed at 240 °C. The electron diffraction pattern was obtained from the dark disk in (b).

in Figs. 5 and 6). Instead, the reflection with a lattice spacing of  $\sim 1.4$  nm appeared, its intensity increasing with the increase of annealing temperature (see the increase in the intensity on peaks indicated by a thick arrow in Figs. 5 and 6). The innermost meridian reflection of the X-ray photograph in Fig. 4(b) is just corresponding to it. The reflection with the lattice spacing of 0.737–0.758 nm, although blurred, was observed in the diffraction profiles of all annealed complex samples. The spacing of the innermost reflection in Fig. 4(c) is 1.4 nm. All inclusion complexes still gave the reflection of the lattice spacing of 1.4 nm even when annealed at 240 °C. The lattice spacing of the reflection is summarized in Table 2. The crystalline form of annealed complexes is considered to be that of  $\gamma$ -CD–PEO proposed by Panovia et al. [28]. This is the hexagonal form in which channel type of complexes is laterally packed in a hexagonal way [38,39].

When annealed at a temperature above 140 °C, inclusion complex samples lost their crystallinity further and became amorphous by annealing at high temperatures, as seen from the X-ray photographs in Fig. 4 and diffraction profiles in Figs. 5 and 6. Inclusion complexes with other polymers also exhibited the similar structural deterioration by desorption of water molecules [20,26]. When annealed samples were exposed to water vapor, crystallinity was recovered, exhibiting the crystalline structure of original sample. Surprisingly, the degree of orientation of crystallites in the original sample was also restored. The original three-dimensional crystalline order of the inclusion complexes is re-constructed only by incorporating water molecules in them. In  $\gamma$ -CD/simple-molecule systems, the similar reversible structural changes were revealed by following the changes in X-ray diffraction patterns in the process of desorption and subsequent absorption of water: when they dried in vacuum, inclusion complexes became amorphous, and the original channel type structure was re-formed after water hydrates were taken in the inclusion complex systems [39]. According to TG measurement of  $\gamma$ -CD–PEA complexes, the second weight loss started at about 180 °C and amounted to 40% at 300 °C (see Fig. 2). Since  $\gamma$ -CD remained un-degraded up to 300 °C, the weight loss implies that PEA chains threading the cavity of  $\gamma$ -CD rings were damaged in annealed complex crystals. However, the necklace framework of the complexes was still retained although array of rings was disordered.

$\gamma$ -CDs were amorphous in drying in vacuum. When amorphous  $\gamma$ -CDs were exposed to air with high humidity, they absorbed water molecules, i.e. with the content of 17 molecules per  $\gamma$ -CD, to crystallize in the complete hydrated form [40]. Using a special method in which the solution of  $\gamma$ -CD in water was poured into acetone, Rusa et al. crystallized  $\gamma$ -CD in the

channel type or columnar structure [41]. When the  $\gamma$ -CD–water complex was heated, it lost water molecules to transform into amorphous. It was found that when amorphous  $\gamma$ -CD was exposed to water vapor, it was re-crystallized into the cage structure [42], i.e. the uncomplete hydrated  $\gamma$ -CD with 14 water hydrates [32]. Thus, in order that the structural transformation occurs reversibly by absorption and desorption of water molecules, it is important that the columnar, or channel type of complex should be retained even though the stacking order of  $\gamma$ -CD rings in it is disordered. Since a simple molecule partly incorporated in cavities of neighboring  $\gamma$ -CDs and shared between them in  $\gamma$ -CD/simple molecule complexes [39] and polymer chains thread through the cavities of  $\gamma$ -CDs to connect them, the original channel type of  $\gamma$ -CD stacking could still be retained in the amorphous complexes even when water molecules are removed. Then, crystalline lateral packing of columns and/or the stacking order of  $\gamma$ -CD rings in a column is disordered.

#### 4.3. Transform of tetragonal form to monoclinic form

In the previous report, it was proposed that the superlattice was involved in the inclusion complex of  $\gamma$ -CD with PEA. There were some ambiguity in the proposition of the superlattice: (1) only  $h00$  and  $0k0$  reflections with  $h$  and  $k$  integers were observed along the  $a^*$  and  $b^*$  axes, respectively, (2) the  $hk0$  diffraction spots were systematically extinct in the diffraction patterns, (3) the  $h00$  and  $0k0$  reflections were spotty and the  $hk0$  reflections are streaky in some case, and (4) the reflections or fine profile attributed to the superlattice were not observed in X-ray diffraction profiles. The diffraction features (1) and (2) are identified in Fig. 7. Even if the superlattice would be set up, the systematic extinction of diffraction spots of the electron diffraction patterns cannot always be explained in terms of the tetragonal crystallographic system. These problems are solved as detailed below.

X-ray diffraction profiles of as-prepared inclusion complexes show no reflections that can be indexed on the basis of the superlattice assumed above. The following was inquired of: electron diffraction patterns were taken in a vacuum and thus the superlattice might be produced at a stage where water molecules as hydrates were removed from the complexes to some extent. A powder sample of complexes was dried in a vacuum at room temperature. Thereafter, X-ray diffraction profile of the dried sample was obtained without exposing to water vapor, using a special technique. The profile thus obtained was compared with that of as-prepared sample in Fig. 3. There were observed no reflections indicating the existence of superlattice. Instead, the 200 reflection of as-prepared complexes is clearly split into three peaks with lattice spacings of 1.29, 1.18 (corresponding to the original reflection) and 1.10 nm (see the reflections indicated by a curly bracket). The lattice spacings of 1.29 and 1.10 nm are just corresponding to those of reflections of the encircled area in Fig. 7(a). It is proved that the crystalline form giving the electron diffraction patterns in Fig. 7 was caused by removal of water molecules from the inclusion complexes in an electron microscope.

Table 2  
Lattice spacings of the main reflection of hexagonal lattice of annealed samples

Ann. temp (°C)	Polymer			
	PEO	PEA	PPG	PIB
140	1.419	1.401	1.452	1.402
240	1.473	1.396	1.439	1.439

It is unknown how much water molecules were removed from the inclusion complex samples. However, it is sure that the amount of loss of water molecules is less than in the case of annealing at high temperatures. In other word, when more water molecules are removed, the hexagonal form is produced as described above.

Taking the above observations into account, we are able to interpret the real diffraction patterns as follows. The reciprocal  $a'^*-b'^*$  net of a monoclinic cell (net A), which is drawn in solid lines in Fig. 10, should be basic, and more than one similar nets, but differently oriented, are superposed on the diffraction pattern. The  $a'^*-b''^*$  net with the common  $a'^*$  axis (net B), drawn in dotted lines, is produced by a mirror symmetry operation with respect to the plane, which is perpendicular to the paper and includes the  $a'^*$  axis. Many spots can be put on the mixed net. However, there are still many diffraction

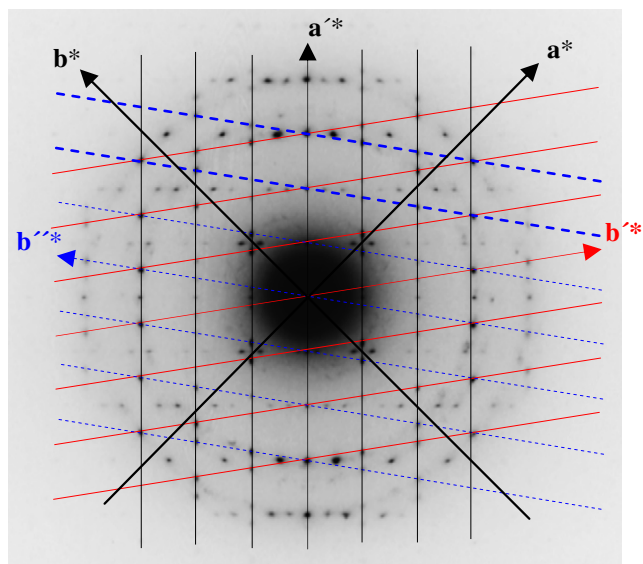


Fig. 10. Relationship of the reciprocal nets of tetragonal and monoclinic lattices to the electron diffraction pattern of  $\gamma$ -CD–PEO complex. The  $a^*-b^*$  net (solid line) shows the reciprocal lattice of tetragonal lattice. The  $a'^*-b''^*$  net (solid line, reciprocal net A) and  $a'^*-b''^*$  net (dotted line, reciprocal net B) correspond to the monoclinic lattice, and they are in mirror relation.

spots not put on the above mixed reciprocal net. Finally, when another mixed net, which is produced by rotating the mixed net by  $90^\circ$  clockwise or anti-clockwise, is superposed on the original mixed net, all the diffraction spots are put on the reciprocal points of the resultant complicated net system. Without setting up a superlattice, the electron diffraction patterns can be interpreted in the combination of four differently oriented monoclinic reciprocal lattices. All the complicated electron diffraction patterns in Fig. 7 are explained in this way. The cell dimensions of the monoclinic unit cell are calculated at  $a = 1.76$  nm,  $b = 1.397$  nm and  $\gamma = 110^\circ$ . It was found out thus that the original tetragonal modification transformed into the monoclinic one when water hydrates were removed by drying in a vacuum at room temperature. Of course, the diffraction profile (b) in Fig. 3 is basically explained in terms of the unit cell.

Fig. 11 shows the tetragonal and monoclinic lattice models, projected on the  $a$ – $b$  basal planes, and the channel type model of inclusion complex of  $\gamma$ -CD. Since the channel type of  $\gamma$ -CD inclusion complexes is stacked laterally in both tetragonal and monoclinic states, the  $c$  cell dimension is considered to be the same in both forms,  $c = 1.472$  nm. In considering the cell size, two inclusion complexes are contained in the tetragonal unit cell and one in the monoclinic unit cell. There is no further information on the crystal symmetry of the tetragonal form. Here, the molecular arrangement corresponding to the crystal structure of  $\gamma$ -CD/simple molecule systems is adopted as depicted in Fig. 11(a): the view of their crystal structure looking down the  $c$  axis [30–34]. The lattice models of Fig. 11(a) and (b) are drawn so as to adjust the orientational relationship between them to that between the tetragonal reciprocal and the monoclinic reciprocal lattices (net A) in Fig. 10. It is found from the above analyses of electron diffraction pattern that the 110 lattice spacing of the tetragonal modification of as-prepared complexes remains unchanged when it transforms into the monoclinic one. Keeping the 110 lattice spacing constant, a model of the monoclinic cell schematized in Fig. 11(b) is set up as follows: rows of projected  $\gamma$ -CD complexes, which are aligned along the (110) plane of the tetragonal lattice, are shifted progressively in the left direction parallel to the (110)

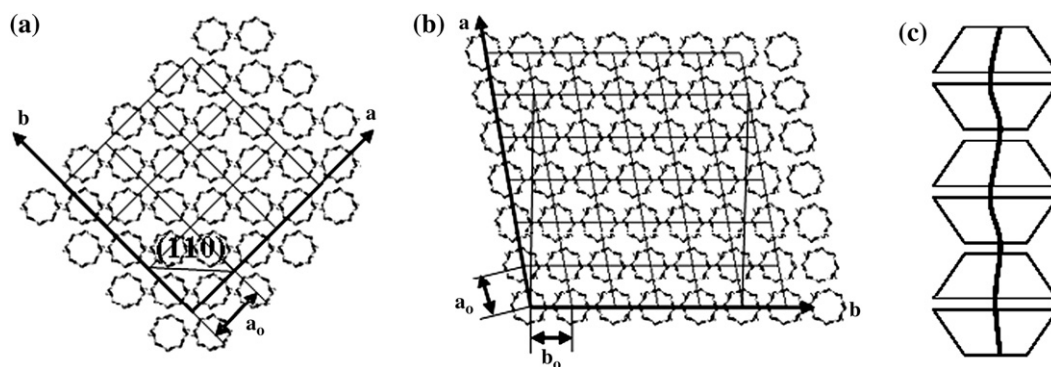


Fig. 11. Packing manners of inclusion complexes of  $\gamma$ -CD, projected on the  $a$ – $b$  basal plane: (a) tetragonal lattice and (b) monoclinic lattice.  $a_0$  and  $b_0$  denote the cell dimensions. The orientational relationship between the two models just corresponds to that between the reciprocal net of tetragonal lattice and the net A in Fig. 10. Circular mark  $\odot$  stands for an inclusion complex projected on the  $a$ – $b$  plane in the direction parallel to the columnar axis. (c) Model of a columnar inclusion complex, in which trapezoids denote  $\gamma$ -CD.  $\gamma$ -CD is stacked in the channel type, alternating the head-to-head and tail-to-tail contacts.

plane, retaining the inter-row distance. Consequently, the oblique, monoclinic lattice is produced as shown in Fig. 11(b). The progressive shift can occur equally in both left and right directions in Fig. 11(a). When the shift in the right direction occurs, the monoclinic lattice with the  $a$  axis inclined at  $80^\circ$  in Fig. 11(b) is given rise to. It gives the reciprocal net B in Fig. 10. Since the crystal lattice has a tetragonal rotational axis normal to the paper, the progressive shifting or shearing of rows of  $\gamma$ -CD inclusion complexes also occurs equally up or down in Fig. 11(a), i.e. in the direction parallel to the  $(\bar{1}10)$  plane. Because of the up and down shifts, other two monoclinic crystal lattices, which differ from the former two in orientation, are produced in the whole crystalline lattice; the two monoclinic lattices cause the mixed reciprocal net produced by  $90^\circ$  rotation as mentioned above.

In the cycle of desorption and absorption of water molecules in inclusion complexes of  $\gamma$ -CD with simple molecules, the X-ray diffraction profiles like the profile of Fig. 3(b) were not observed [39,41,42]. This suggests that inclusion complexes with simple molecules could not hold water molecules in them at an amount where the monoclinic form could be fixed to be stable. In complexes of  $\gamma$ -CD with PEG, the monoclinic form was not always observed independent of the molecular weight. In concluding, the formation of monoclinic form might depend on the molecular length of included guest molecules. This will be described in future.

#### 4.4. Streaky electron diffraction pattern

In the previous paper [29], the streaky reflections are not explained on the basis of two-dimensional paracrystalline disorder, because if the disorder is two-dimensional, the diffraction spots should spread two-dimensionally. It is also true at the present case. As seen in the electron diffraction patterns in Figs. 7, 9 and 10, some reflections are extended one-dimensionally, i.e. in the direction perpendicular to the  $a'^*$  axis of the monoclinic lattice (see Fig. 10). Such streaky

reflections were observed in many polymer single crystals [43–46]. They are explained on the basis of the growth mechanism of crystals: stacking faults are repeatedly introduced into crystals and results in the reduction of coherent crystallite size. The diffraction features were actually computer-simulated on the stacking fault model [44]. The stacking faults were directly resolved in molecular dimension by high-resolution electron microscopy [46]. Quite recently, the size reduction was observed in poly(vinylcyclohexane) (PVCH) single crystals by using the dark field electron microscopy [47]. Fig. 12 shows a similar kind of electron diffraction pattern, in which reflections are extended parallel to either of the main reciprocal axes of the  $a^*$  and  $b^*$  axes. The streaking or broadening features of reflections of Figs. 7 and 12 are quite similar. In Figs. 7 and 12, the streaky reflections are not expanded in the direction normal to their streaking direction. It is understood from diffraction theory that the crystalline blocks regularly grow to a large extent in the normal direction. In Ref. [47], dark field electron microscopy proved it: single crystals consist of thin extended blocks and reflections extend in the direction normal to the length of thin blocks. Now let us consider the case that shearing occurs alternating its direction left and right in Fig. 11(a). In such a case, monoclinic crystalline slices are stacked in layers, alternating the oblique direction of the  $a$  axis, as schematized in Fig. 13. As a result of frequent change in the shearing direction, layers with different thickness are stacked in the direction normal to the shearing direction. At the boundaries between neighboring layers, twinning relation holds. Even in the layered structure, the extent of coherent size of crystallite in the direction normal to the  $b$  axis, i.e. in the  $a'^*$  direction, remains unchanged because the continuity of 100 lattice spacing of the monoclinic lattice still holds across the twin boundary (see Fig. 13). This shows that the  $h00$  reflection of monoclinic lattice is not affected and kept spotty even when the crystalline structure is disordered. However, in the direction off from the  $a'^*$  axis, the continuity of same lattice plane is interrupted at the twinning boundaries,

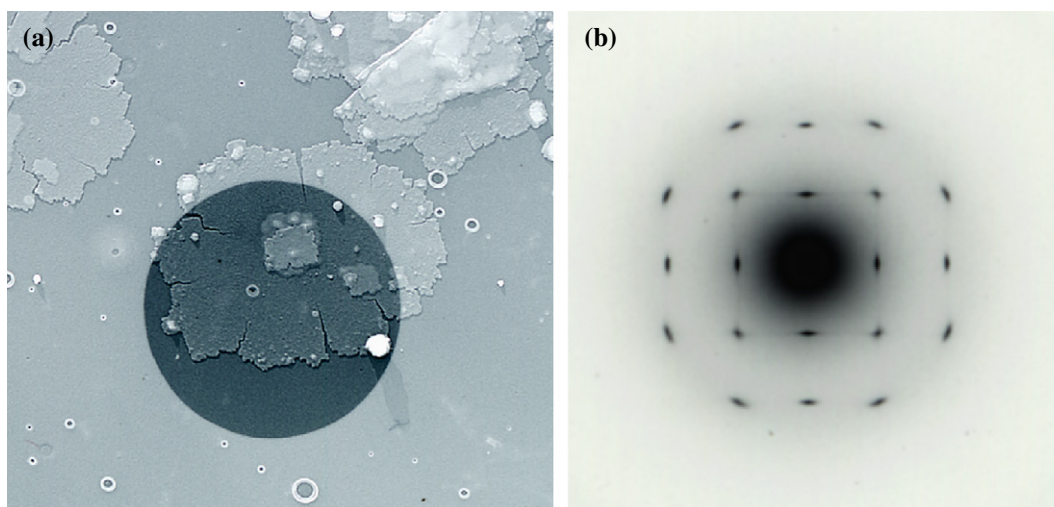


Fig. 12. (a) Electron micrograph of lamellae of poly(vinylcyclohexane) and (b) the electron diffraction pattern corresponding to a dark disc in (a). The lamellae were grown from the dilute solution in diphenyl ether.

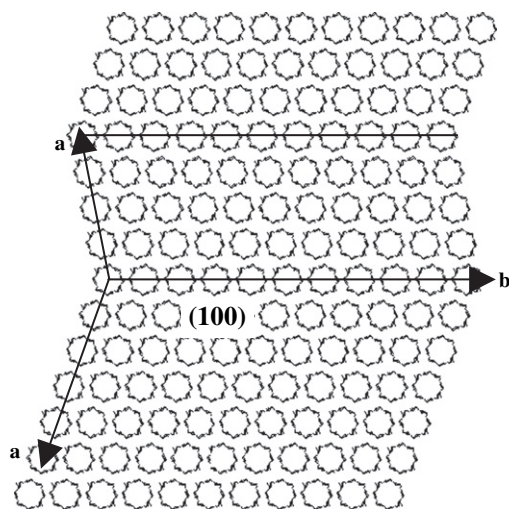


Fig. 13. Stacked layers in the monoclinic lattice, produced by changing the shearing direction left and right, i.e. in the  $[110]$  direction along the  $(110)$  plane of the tetragonal lattice. The mirror relation between neighboring layers holds with respect to the  $(100)$  plane of monoclinic lattice.

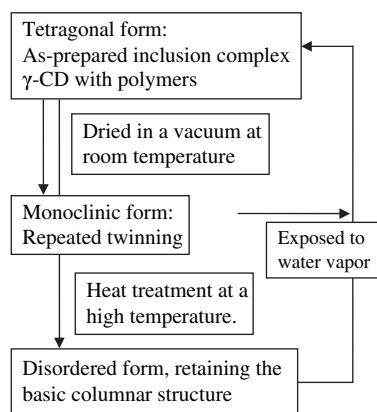


Fig. 14. Scheme of transformation between different crystalline forms of inclusion complexes of  $\gamma$ -CD with polymers, depending on the content of water molecules in their crystal lattice.

leading to the reduction of crystallite size, and hence the  $hk0$  reflection could be diffused and extended. The layered structure would be produced equally by shearing of  $\gamma$ -CD rows in the  $[110]$  direction of the original tetragonal lattice. Thus, it is explained, though qualitatively, that the reflections on the  $h00$  and  $0k0$  reflections are spotty and  $hk0$  reflections are streaky in some case.

## 5. Conclusion

It was found that water molecules were inevitable to form crystalline inclusion complexes of  $\gamma$ -CD with various polymers. There are three modifications depending on the content of water in the complexes. Which crystalline form is stable is dependent on the content of water hydrates in the complexes. The relationship between the modification and the content of water molecules is summarized, though qualitatively, as described in Fig. 14.

In order to elucidate the mechanism of transformation, depending on the content of water, it is needed to make more clear the crystalline structure of the inclusion complexes of the tetragonal, hexagonal and monoclinic modifications.

## Acknowledgement

Authors are grateful to Prof. Y. Yoshimura and his co-workers, Ritsumeikan University, for their assistance in using the reading facilities of X-ray imaging plate data.

## References

- [1] Szejtli J. *Pure Appl Chem* 2004;76:1825–45.
- [2] Bonacchi D, Caneschi A, Dorignac D, Falqui A, Gatteschi D, Rovai D, et al. *Chem Mater* 2004;16:2016–20.
- [3] Harada A, Kamachi M. *Macromolecules* 1990;23:2821–4.
- [4] Harada A, Li J, Kamachi M. *Nature* 1992;356:325–7.
- [5] Harada A, Adachi H, Kawaguchi Y, Kamachi M. *Macromolecules* 1997;30:5181–2.
- [6] He L, Huang J, Chen Y, Xu X, Liu L. *Macromolecules* 2005;38:3845–51.
- [7] Dong T, He YH, Shin K, Inoue Y. *Macromol Biosci* 2004;4:1084–91.
- [8] Peet J, Rusa CC, Hunt MA, Tonelli AE, Balik CM. *Macromolecules* 2005;38:537–41.
- [9] Harada A, Li J, Suzuki S, Kamachi M. *Macromolecules* 1993;26:5267–8.
- [10] Harada A, Li J, Kamachi M. *Nature* 1994;370:126–8.
- [11] Harada A, Okada M, Li J, Kamachi M. *Macromolecules* 1995;28:8406–11.
- [12] Harada A, Nishiyama T, Kawaguchi Y, Okada M, Kamachi M. *Macromolecules* 1997;30:7115–8.
- [13] Mishra M, Edwards JC, Subramanian P, Pugliese RD. *Des Monomers Polym* 1998;1:225–36.
- [14] Lu J, Shin ID, Nojima S, Tonelli AE. *Polymer* 2000;41:5871–83.
- [15] Okumura H, Okada M, Kawaguchi Y, Harada A. *Macromolecules* 2000;33:4297–8.
- [16] Wei M, Tonelli AE. *Macromolecules* 2001;34:4061–5.
- [17] Lu J, Mirau PA, Tonelli AE. *Macromolecules* 2001;34:3276–84.
- [18] Porbeni FE, Edeki EF, Shin ID, Tonelli AE. *Polymer* 2001;42:6907–12.
- [19] Topchieva IN, Panova IG, Popova EI, Matukhina EV, Grokhovskaya TE, Spiridonov VV, et al. *Polym Sci* 2002;44:588–96.
- [20] Li J, Yan D, Jiang X, Chen Q. *Polymer* 2002;43:2625–9.
- [21] Li J, Mai Y, Yan D, Chen Q. *Colloid Polym Sci* 2003;267–74.
- [22] Rusa CC, Wei M, Shuai X, Bullions TA, Wang X, Rusa M, et al. *J Polym Sci Part B Polym Phys* 2004;42:4207–24.
- [23] Hernández R, Rusa M, Rusa CC, López D, Mijangos C, Tonelli AE. *Macromolecules* 2004;37:9620–5.
- [24] Michishita T, Takashima Y, Karada A. *Macromol Rapid Commun* 2004;25:1159–62.
- [25] Rusa CC, Rusa M, Comez M, Shin ID, Fox JD, Tonelli AE. *Macromolecules* 2004;37:7992–9.
- [26] Uyar T, Rusa CC, Hunt MA, Aslan E, Hacaloglu J, Tonelli AE. *Polymer* 2005;46:4762–75.
- [27] Hwang HS, Lee MY, Jeong YT, Hong S-S, Gal Y-S, Lim K-T. *Ind Eng Chem Res* 2006.
- [28] Panovia IG, Gerasimov VI, Kalashnikov FA, Topchieva IN. *Polym Sci Ser B* 1998;40:415–9.
- [29] Ohmura M, Kawahara Y, Okude K, Hasegawa Y, Hayashida M, Kurimoto R, et al. *Polymer* 2004;45:6957–75.
- [30] Linder K, Saenger W. *Biochem Biophys Res Commun* 1980;92:933–8.
- [31] Kamitori S, Hirotsu K, Higuchi T. *J Am Chem Soc* 1987;109:2409–14.
- [32] Harata K. *Bull Chem Soc Jpn* 1987;60:2763–7.
- [33] Kamitori S, Hirotsu K, Higuchi T. *Bull Chem Soc Jpn* 1988;61:3825–30.

- [34] Ding J, Steiner T, Saenger W. *Acta Crystallogr* 1991;B47:731–8.
- [35] Steiner T, Saenger W. *Acta Crystallogr* 1998;B54:450–5.
- [36] Meier MM, Luiz MTB, Szpoganicz B, Soldi V. *Thermochim Acta* 2001;375:153–60.
- [37] Giordano F, Novak C, Moyano JR. *Thermochim Acta* 2001;380:123–51.
- [38] Takeo K, Kuge T. *Agric Biol Chem* 1970;34:568–74.
- [39] Uyar T, Hunt MA, Gracz HS, Tonelli AE. *Cryst Growth Des* 2006;6: 1113–9.
- [40] Nakai Y, Yamamoto K, Terada K, Sasaki I. *Yakugaku Zasshi* 1986;106: 420–4.
- [41] Rusa CC, Bullion TA, Fox J, Porbeni FE, Wang X, Tonelli AE. *Langmuir* 2002;18:10016–23.
- [42] Hunt MA, Rusa CC, Tonelli AE, Balik CM. *Carbohydr Res* 2005;340: 1631–7.
- [43] Lovinger AJ, Davis DD, Lotz B. *Macromolecules* 1991;24: 552–60.
- [44] Tsuji M, Okihara T, Tosaka M, Kawaguchi A, Katayama K. *MSA Bull* 1993;23(1):57–65.
- [45] Lovinger AL, Lotz B, Davis DD, Padden Jr FJ. *Macromolecules* 1993;26:3494–503.
- [46] Hamada N, Tosaka M, Tsuji M, Kohjiya S, Katayama K. *Macromolecules* 1997;30(22):6888–92.
- [47] Alcazar D, Ruan J, Thierry A, Kawaguchi A, Lotz B. *Macromolecules* 2006;39:1008–19.